Clays and Clay Minerals (2025), **73**, e25, 1–12
doi:10.1017/cmn.2025.10012

Original Paper

The making of kaolinite suspension time-dependent in the structural rejuvenation mode – the face charge hypothesis

Yee-Kwong Leong[1] and Peta L. Clode[2]

[1]Department of Chemical Engineering, The University of Western Australia, 35 Stirling Highway, Crawley, WA 6009, Australia and [2]Centre for Microscopy, Characterization and Analysis, The University of Western Australia, 35 Stirling Highway, Crawley, WA 6009, Australia

Abstract

The physical property requirements for kaolinite suspensions to display time-dependent structural rebuilding or rejuvenation behavior are the same as required by smectite gels such as hectorite and Na-montmorillonite (NaMnt), a rare discovery linking the two types of clay. A holistic framework for predicting clay gel behavior based on the clay physical properties such as charge, crystal structure, and mineralogy, may emerge and was the ultimate goal of this research. A structural rejuvenation process during both ageing and stepdown shear rate modes was postulated to require that the silica and alumina faces of the kaolinite platelets be negatively charged to produce a strong electric double layer (EDL) repulsion in all face-face configurations. This is needed to slow down the (+)edge to (–)face bonding process to produce the time-dependent behavior. Currently, the unlike charge attraction between the silica and alumina faces makes the structural rebuilding process of a pre-sheared kaolinite suspension too fast to be observable. Two methods of making the alumina face negatively charged, i.e. the use of adsorbed $P_2O_7^{4-}$ and high pH, did indeed produce the time-dependent behavior for both KGa-1b and KGa-2 suspensions, thus validating the proposed hypothesis. The KGa-1b with a lower content of octahedral positive layer charge required less $P_2O_7^{4-}$ and a lower pH to achieve the desired outcome. Addition of 0.002 M NaCl to the high pH-treated KGa-2 suspension hastened the structural rejuvenation process and increased the aged gel strength. The oscillatory behavior in the stepdown shear stress at low pH was due to layer agglomerates formed by (+)face to (–)face attraction. Bulky layered agglomerates were reduced markedly by both the $P_2O_7^{4-}$ and high pH treatments. The knowledge gained was applied successfully to make clay-rich iron ore tailings time-dependent in both the ageing and stepdown shear rate modes.

Keywords: bentonite; pH; positive layer charge; pyrophosphate; salt; thixotropy

(Received: 18 February 2025; revised: 07 June 2025; accepted: 11 June 2025)

Introduction

Background

Unlike smectite gels of NaMnt and hectorite, pre-sheared kaolinite suspensions at their natural pH do not display time-dependent behavior in the structural rebuilding or rejuvenation phase during ageing (Leong et al., 2021a) and in the stepdown shear rate mode (Leong, 2024). Upon uncovering the physical mechanism involved and the surface properties required for such behavior with the smectite gels, the making of kaolinite suspensions time-dependent in this mode became a real possibility and the success of doing so was a significant validation of the scientific principle involved or uncovered. This validation will be strengthened here repeatedly with more tests and different materials.

For platelet-type clay gels of NaMnt and hectorite, a strong electric double layer (EDL) repulsive interaction between platelets in the face-face configuration was responsible for the time-dependent behavior being observable in the structural rejuvenation process of pre-sheared gels (Leong and Clode, 2023; Leong, 2024). This strong repulsion is needed to slow down the bonding process in the edge-face configuration during the structural development process. In the ageing test, the gel strengthens spontaneously with time at rest. The gel strength in this test is often measured by the shear yield stress. For this gel to flow, the imposed shear stress must exceed this yield stress. In the stepdown shear rate test, the gel will display EDL repulsive force-control time-dependent behavior in the stepdown shear stress response. This time-dependent behavior is characterized by the shear stress increasing immediately upon stepdown and continues until it reaches an equilibrium or steady state. A stronger EDL repulsive force is needed, to counter the imposed shear force while still strong enough to disrupt the flow-aligned platelets to form a stronger structure. Like ageing, this temporal shear stress increase represents an increasingly stronger structure being formed. In the semectite gels, the strong EDL face-face repulsion is due to the silica faces of the NaMnt and hectorite platelets being highly negative. Laponite and bentonite gels also displayed such time-dependent behavior (Leong et al., 2021b; Leong and Clode, 2023).

Corresponding author: Yee-Kwong Leong; Email: yeekwong.leong@uwa.edu.au
Cite this article: Leong Y.-K., & Clode P.L. (2025). The making of kaolinite suspension time-dependent in the structural rejuvenation mode – the face charge hypothesis. *Clays and Clay Minerals* **73**, e25, 1–12. https://doi.org/10.1017/cmn.2025.10012

Kaolinite, as a 1:1 clay mineral, consists of an alumina sheet bonded to a silica sheet. Strong EDL repulsive interaction does occur between silica faces and between alumina faces at close contact, but the interaction between silica and alumina faces is attractive (Leong et al., 2021c). Both the silica and alumina faces were reported to contain pH-dependent charge groups, in addition to the permanent layer charge (Kumar et al., 2021). Silica has a point of zero charge (pzc) at pH ~2 while that for alumina is ~9.5 (Kosmulski, 2023). The pH-dependent charge is, therefore, negative at all pH values >2 for the silica face (Franks, 2002). So silica and alumina face-face attraction can occur over a wide pH range of 2–10 and hence the formation of layered agglomerates (Gupta et al., 2011; de Bono & McDowell, 2023) occurs at its natural pH of ~5. A kaolinite suspension was observed to display EDL repulsive force-control time-dependent behavior in the stepdown shear stress response when treated with adsorbed $P_2O_7^{4-}$ additive to increase the negative charge density of the clay platelets (Leong, 2024). One of the aims of the present study was to validate conclusively that the original hypothesis proposed (Leong, 2024) is correct, i.e. to show that high pH treatment can impart similar EDL repulsive force-control time-dependent properties to the kaolinite suspension. The pH employed must be such that the alumina face is negatively charged. This display of EDL repulsive force-control time-dependent behavior should also occur in the ageing mode, which will be evaluated as a further proof. As a further consolidation of the validation, a kaolinite-rich mineral waste product will be made to display time-dependent behavior in the structural rejuvenation mode. One such product is a kaolinite-rich iron ore tailings (Leong, 2021).

Other related aspects included in this study are the effects of the positive layer charge on the amount of $P_2O_7^{4-}$ additive and pH increase needed for the display of such time-dependent behavior. Two kaolinites from the Source Clays Repository of The Clay Minerals Society, USA, with different positive layer charge in the alumina octahedral sheet were used. The state of the layered agglomerates on the flow properties of one of these kaolinites was also included.

With kaolinite suspensions treated to make the alumina surface net negative, many platelets will be released from the layered agglomerates to form the network structure with the (+)edge-(–)face bonds. If high pH treatment is employed, this required the platelet edge to remain positively charged. Permanent positive charges at the edge can occur if some of the edge AI(III) are isomorphically substituted by Ti(IV) or Si(IV). Ti(IV) is present in the two source kaolinites. According to the chemical composition of the unit strucuture, all the Ti(IV) are located in the alumina octahedral sheet and the amount present is exactly equal to the positive layer charge of the octahedral sheet (CMS, 2024). It is well known that the crystal size formed is limited by the concentration of defects and they tend to be located at the crystal edge. The pH-dependent positive charges are also present. With a Mg substituted Al site at the edge of a NaMnt platelet, the Mg-$(OH_2)_2$ group will remain positively charged at pH >13 as its computed pKa value was as high as 13.2 (Liu et al., 2013). Trace amounts of Mg(II) are present in the octahedral sheet of the high defect KGa-2 (CMS, 2024).

The study of dried and wet kaolinite properties has spanned hundreds if not thousands of years because of its importance in pottery making. Yet, new properties and behavior continue to be uncovered. Kaolinite is one of the most abundant clay minerals on earth. Its importance in geology, agriculture, and civil engineering building foundation is indisputable. It also has many commerical uses (Harvey and Murray, 1997; Murray, 2000) such as a source of aluminum, brick, ceramics or porcelin ware, paper coating material, and fillers in many products. It has very interesting interfacial properties which control all its behavior in the wet state (Bergaya et al., 2006) and the present study is a good example of that. It can also pose significant problems in mining and mineral processing, and in handling and safe storage of minewaste tailings (Liu et al., 2020). Microstructure or fabric of wet kaolinite determines many physical properties such as soil permeability and strength, and flow and dewatering behavior of suspensions (Palomino and Santamarina, 2005; Liu et al., 2020). Interfacial chemistry controls many kaolinite suspension properties such as dispersibility and rheology (Schofield and Samson, 1954; van Olphen, 1963; Swartzen-Allen & Matijević, 1974; Rand and Melton, 1977). However, many surface-suspension property relationships have yet to be discovered. When and how wet kaolinite displayed time-dependent behavior have direct implications in many of these applications.

Theory

For interaction between two similarly charged parallel plates, the EDL interaction energy per unit area, W_{EDL}, is given by (Israelachvili, 1992):

$$W_{EDL} = \frac{64kT\rho_\infty}{\kappa} \tanh^2\left[\frac{ze\psi_o}{4kT}\right] * e^{-\kappa H} \left(\mathrm{Jm}^{-2}\right) \quad (1)$$

where ψ_o is the surface potential (mV); κ^{-1} is the EDL thickness or surface charge shielding length; ρ_∞ is the number density of ions in the bulk; e is the electronic charge; H is the face-face separation distance; k is the Boltzmann constant; T is the temperature; and z is the valence of the ions. The strength of the EDL repulsive force is, therefore, dependent on the same factors; ψ_o, κ^{-1}, and H.

The EDL thickness or Debye length is given by:

$$\kappa^{-1} = \left(\frac{\varepsilon_o \varepsilon kT}{\sum_i \rho_{\infty,i} e^2 z_i^2}\right)^{\frac{1}{2}} (\mathrm{m}) \quad (2)$$

where ε_o is the permittivity in free space; ε is the relative permittivity; $\rho_{\infty,i}$ is the number density of i^{th} ion in the bulk; and z_i is the valence of i^{th} ion.

The corresponding van der Waals interaction energy per unit area is:

$$W_{VdW} = -\frac{A_{131}}{12\pi H^2} \left(\mathrm{Jm}^{-2}\right) \quad (3)$$

where A_{131} is the Hamaker constant of the clay minerals in water. The negative sign denotes attractive interaction energy. The van der Waals (Vdw) attractive interaction energy or force becomes infinite if the separation distance of the interacting faces H=0. For layered agglomerates, H would be close to zero if their interacting surfaces are molecularly smooth. This attractive interaction is likely to be weak in the edge-face configuration as the interaction area is quite small and edges are uneven or jagged. The unlike charge attraction provides the strength of the edge-face bond.

When the EDL repulsive interaction in the face-face configuration is very strong, the interacting platelets will oscillate in this strong force until they get into a low energy edge-face configuration to bond. The platelet-platelet interaction at the edge-face angle of 90° is one such low energy configuration. This slows down the bonding process

and hence the display of the time-dependent behavior in the structural rebuilding or rejuvenation mode. More lower energy edge-face bonding configurations are created at higher salt concentration (0.01–0.1 M KCl) by the thinner EDL. In hectorite gel, time-dependent behavior in the stepdown shear stress response was not seen as the bonding speed has become too fast (Leong and Clode, 2024).

Materials and methods

The KGa-1b and KGa-2 samples from the Source Clays Repositiory of The Clay Minerals Society, USA, were used. The chemical formula of the unit structure of KGa-1b is $(Mg_{.02}$ C–$a_{.01}$ $Na_{.01}$ $K_{.01})$ $[Al_{3.86}$ $Fe(III)_{.02}$ Mn_{tr} $Ti_{.11}][Si_{3.83}$ $Al_{.17}]O_{10}(OH)_8$ and that of KGa-2 is $(Ca_{tr}$ $K_{tr})[Al_{3.66}$ $Fe(III)_{.07}$ Mn_{tr} Mg_{tr} $Ti_{.16}][Si_{4.00}]O_{10}(OH)_8$. The KGa-1b is a low-defect or high-crystallinity kaolinite while the KGa-2 is a low-crystallinity kaolinite. The amount of impurities in both kaolinite is the same, ~7%. Their respective specific areas of 9.8 and 18.4 m^2 g^{-1} were measured independently using a nitrogen adsorption method. A Micromeritics Tristar (Micromeritics Instrument Corporation, USA) was used and only adsorption data that obeyed the Brunauer, Emmett and Teller (BET) model were specifically verified and then used to obtain the specific area. KGa-2 has an octahedral layer charge of +0.16 e and a tetrahedral charge of 0.0 e. The permanent positive charge in the alumina octahedral sheet is due to the isomorphic substitution of Al^{3+} by Ti^{4+}. For KGa-1b, the octahedral charge is lower, +0.11 e and the tetrahedral charge is –0.17 e. Most of these data are freely available (CMS, 2024). Both the silica and alumina layers also contain pH-dependent surface charges (Kumar et al., 2021). The point of zero charge (pzc) was reported to be at pH ~3 for the KGa-1b and at pH ~4 for the KGa-2 (Au et al., 2015). A kaolinite-rich iron ore tailing with its mineralogy specified in Leong (2021) was also evaluated for this time-dependent behavior conversion. The alumina layer of both source kaolinite possessed permanent positive charges. To achieve the objective of making this alumina layer net negative, a complete neutralization of these permanent and pH-dependent positive charges was required.

Analytical grade (AR), 99.7% pure NaCl used was sourced from Chem-Supply Pty Ltd, Australia. AR grade, 99.0% pure $Na_4P_2O_7.10H_2O$ was purchased from Sigma Aldrich. The dosage of $P_2O_7^{4-}$ added to the kaolinite suspensions is expressed on a dry weight basis in percent (wt.%), i.e. g $P_2O_7^{4-}$ per 100 g clay solids. AR grade, 99.8–102% pure 8 M NaOH from Fluka was used to increase the pH of the suspensions.

The suspensions with the desired loadings of solids were prepared by sonicating known amounts of kaolinite and deionized (DI) water with a high-intensity ultrasonic probe with a half inch horn operated at an amplitude of 60%. A Vibra Cell VCX600 sonic probe (Sonics & Materials Inc., USA) with a power of 600 W was used. To make a 40 wt.% solids KGa-1b suspension, for example, 40 g of kaolinite was mixed and sonicated with 60 g of DI water. A sonication time of 2–3 min was sufficient to produce a smooth homogeneous suspension. The solids concentration determined by drying a sample in an oven at 105°C for at least 3 h was 39.98 wt.%. The amount of dissolved salt in the suspension was measured with an Orion 4-star conductivity meter (Thermo Scientific, USA). The pH was measured with an Orion Star A211 pH meter (Thermo Scientific, USA). The KGa-1b and KGa-2 suspensions displayed a natural pH of 5.3 and 4.5 (Leong et al., 2021a). Brookfield vane viscometers RVDV-II+PRO and LVDV-II+PRO (AMETEK Brookfeld, Middleboro, MA, USA) with different spring constants were used to measure the yield stress during ageing. In the ageing test, the suspension (50–70 g) was first sheared with a spatula for 2 min in a mixture of circular and side-to-side motions to break down the structure. Immediately after that, it was allowed to rest or age undisturbed. At each pre-determined interval of ageing, the yield stress was measured. Each measurement was conducted in an area not disturbed by a previous measurement. For the stepdown shear rate test, an Anton Paar MCR72 rheometer (Anton Paar GmbH, Graz, Austria) was used. A 1° cone-and-plate measuring geometry was chosen and this was to ensure that the suspension experienced the same shear rate $\dot{\gamma}$ everywhere in the gap. In this test, the sample suspension was sheared for 5 min at $\dot{\gamma}$ of 1000 s^{-1} followed immediately by a further 10 min at 10 s^{-1}. For both tests, the intial state of the suspension at the start of the structural rebuilding process was well-defined. In ageing, the initial state structure would be at an equilibrium breakdown state where the yield stress does not change with further stirring time. In the stepdown shear rate test, the platelets should be aligned in the flow direction by the high shear rate of 1000 s^{-1} before the start of the structural rebuilding process at 10 s^{-1}. The sample suspension was usually stirred before being placed in the rheometer and this was to help the suspension attain the equilibrium state much sooner, before the end of the 5 min of shearing at 1000 s^{-1}. For the suspension of clay-rich iron ore tailings, coarse particles greater than 150 μm were sieved out for the stepdown shear rate test.

To avoid ice crystal formation distorting the suspension microstructure (Au et al., 2015; Leong et al., 2021c), the samples for imaging were first subjected to a high pressure of 2000 bar and then frozen rapidly at a rate of 25,000°C s^{-1} employing a Leica EMPact2 High Pressure Freezer. After that, the samples were sublimated and coated with a 7–8 nm thick Pt film using a Leica MED0200 cryo preparation system. The microstructure was imaged with a Zeiss Supra55 feld emission SEM (FESEM) fitted with a Leica EM VCT100 cryo and anti-contamination system (Carl Zeiss Microscopy GmbH, Jena, Germany). With the latest kaolinite suspensions, the same high-pressure freezer was used in the sample preparation. However, a Leica ACE600 system was used for the sublimation and Pt coating. Only the top water layer, micron-thick, was sublimated. The new images were captured with a JEOL IT800HL FESEM fitted with a Leica VCT500 cryosystem (JOEL Ltd, Japan).

The particle-size distribution was characterized using a Malvern Mastersizer 3000E (Malvern Panalytical, UK).

Results and Discussion

KGa-2 kaolinite suspension

Stepdown shear rate and microsturcture: pH and adsorbed $P_2O_7^{4-}$ effects

At pH 4.53 (natural pH) and 6.28, the 31.4 wt.% KGa-2 kaolinite suspension displayed oscillatory behavior in the stepdown shear stress response at 10 s^{-1} (Fig. 1a). At pH 4.53, the shear stress upon stepdown showed a sharp drop initially from 300 to ~350 s. This was followed by the display of oscillatory behavior. The oscillations, some with close double peaks, did not have a very regular period. These close double peaks were likely from the same half-cycle. The magnitude of the average shear stress displayed a slightly increasing trend. For the suspension at pH 6.28, the period of oscillation was much more regular, spanning over a long shearing time. The average shear stress appeared to be constant from 400 s onwards. The magnitude of the average stepdown shear stress was similar at

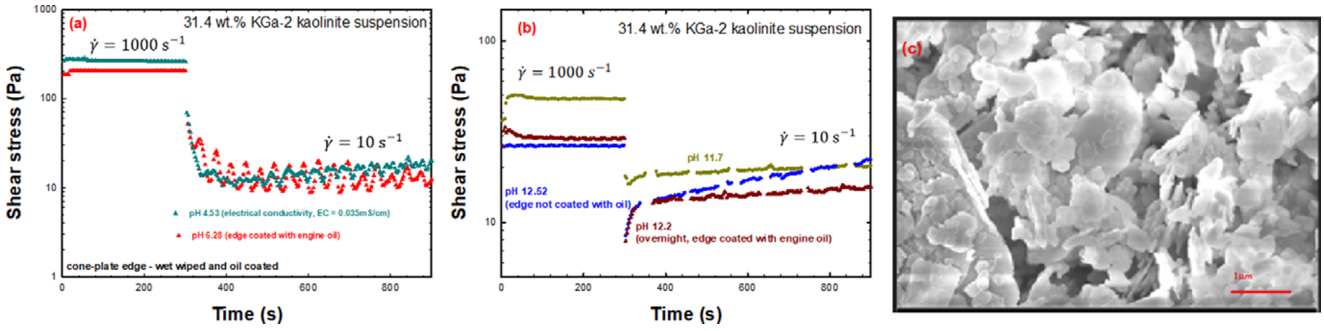

Figure 1. Effect of pH on the stepdown shear rate behavior of 31.4 wt.% KGa-2 kaolinite suspensions at (a) low pH, and (b) high pH, and (c) the microstructure of 26.5 wt.% KGa-2 suspension showing layered agglomerates forming the network. This microstructure image was captured a few years ago using a cryo-SEM FESEM technique. The more recent microstructure was captured using the same techuique but with more advanced cryo-SEM FESEM equipment. The procedure also involved the avoidance of ice crystal forming. Note that not all kaolinite suspensions displayed oscillatory behavior in the stepdown shear stress (Leong, 2024).

the two pH values. Both gels were sheared to an equilibrium state just before stepdown, so the initial state for the structural rejuvenation process was well defined.

At high pH, particularly the suspension at pH 12.5, the stepdown shear stress response (Fig. 1b) displayed classical EDL repulsive force-control time-dependent behavior. The shear stress increased sharply initially and then more gradually with time. The oscillatory behavior observed at the lower pH levels was no longer visible. High pH treatment did indeed produce the time-dependent behavior as postulated. Both the silica and alumina face charge became net negative. Hence, all face-face interactions, including that between alumina and silica, were then repulsive. Although the equilibrium shear stress at 1000 s^{-1} was much lower than that at the low pH level, the magnitude of the stepdown shear stress was as high. The sample at pH 12.5 after resting overnight continued to display similar time-dependent behavior. The pH, however, has decreased to 12.2. The reproducibility of the stepdown shear stress response was extremely good for the first 150 s of shearing. However, the sample at pH 12.5 displayed a sharper increase in the shear stress after that. Water evaporation of the sample during the characterization could be the cause. No oil was used to coat the exposed sample surface at the edge of the cone-and-plate. The sample at pH 12.2 with oil coating showed a much more gradual increase in the stepdown shear stress. The difference in the stepdown shear stress at the end of shearing between them was still relatively small. This value for the sample with oil coating was 71% of that without. The initial stepdown shear stress was also smaller, 94% of that with no coating.

For the gel at pH 4.53, the sharp initial decrease in the stepdown shear stress (Fig. 1a) was due to rapid aggregation to form layered agglomerates reducing the number of colloidal particles contributing to the shear stress or viscosity (ratio of shear stress to shear rate). These layered agglomerates in the microstructure (Fig. 1c) were clearly present. They were very compact. The unlike charge face-face attraction between the silica and alumina was generally very strong when their respective surface charge densities were high. A range of factors affect this bond strength. These are: (1) the area of face-face interaction; (2) smoothness of the interacting surface; and (3) the distance of interaction. The speed of the bonding should be very fast when the layers are within range of this attractive force. Repulsive interaction imparted by neighboring platelets is expected to be weak as the layers are usually more distantly located. The initial depletion of individual kaolinite layers will be very rapid because 50% of all face-face encounters are between silica and alumina. At pH 6.28, this silica-alumina face-face attraction should be weaker as the positive charge density of the alumina will be lower. The depletion of the number of individual layers by aggregation will, therefore, occur to a smaller degree and this accounts for the smaller decrease in the initial stepdown shear stress. Smaller layered agglomerates are expected to form. The imposed shear will also moderate the agglomerate size by breaking up the weaker large agglomerates. At rest, the network structure is formed by these layered agglomerates interacting attractively (Fig. 1c). The jagged nature of the layered agglomerates means that bonding between agglomerates can be easily accomplished. It only takes a jagged edge of one to meet an oppositely charged face of another. The formation of layered agglomerates depletes the concentration of attractive particle interaction in the edge-face configuration responsible for the gel strength. This explains the much higher solids loading needed for the kaolinite suspension compared with NaMnt gel, i.e. ten times as much, to produce a significant yield stress.

Two crucial pieces of evidence supported the premise that the layered agglomerates were responsible for the oscillatory behavior in the stepdown shear stress at low pH. As pointed out, this oscillatory behavior disappeared when the unlike charge face-face attraction between silica and alumina was no longer present. This occurred at high pH when all the face-face interactions were repulsive. This also occurred when all the fixed charge interactions between surfaces were made unimportant by using high salt concentration to shield the surface charge. The absence of oscillatory behavior in the stepdown shear stress (Fig. 2) was displayed by a 31 wt.% KGa-2 suspension treated with 0.5 M KCl. The stepdown shear stress reached a steady value after only 50 s of shearing for all three samples characterized. The initial stepdown shear stress was higher than this steady-state value for all samples, including the one with no added salt, also shown in Fig. 2 for comparison. The absence of oscillatory behavior was more clearly seen (Fig. 2) for the salt-treated sample with oil coating. The face and edge charges were completely shielded by the high ionic strength. Only one colloidal force was important in this situation, i.e. the van der Waals attractive force. In the test, the 5 min of shearing at 1000 s^{-1} would have produced many individual clay platelets and thin layered agglomerates. Upon stepdown, these particles would interact attractively via van der Waals attraction to form the aggregates. These aggregates would be weaker and less dense compared with the layered agglomerates.

Evidence of the large aggregate formation at low shear rates was observed in a two roll-mill mixing experiment. A freshly prepared homogeneous KGa-2 suspension with an appreciable yield stress kept in a screw-cap container was rolled for ~4 h. A hollow well at

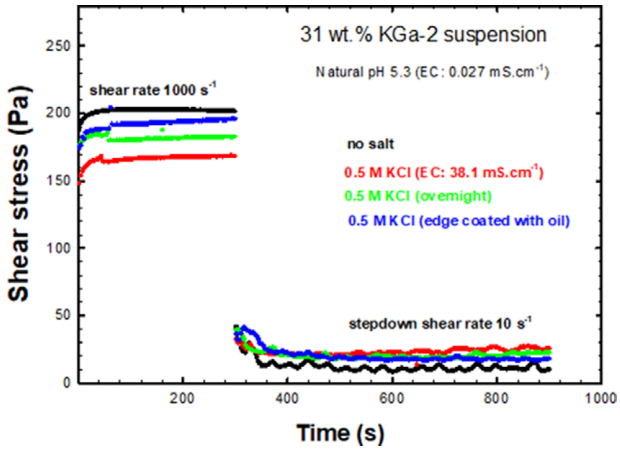

Figure 2. Effect of high salt concentration on the stepdown behavior of 31 wt.% KGa-2 suspension. A suspension was prepared and the stepdown behavior was characterized immediately and overnight. The gel with oil coating applied at the edge of the cone-and-plate to prevent evaporation showed a more consistent stepdown shear rate behavior with much less undulation or variablility in the set of data. Drying for 15 min during characterization can increase the solids by 1–2%.

the center of the container was formed by the rolling motion as much of the suspension was pushed against the container wall. The suspension surface in this well, which experienced a very low shear rate, showed the presence of lumps, indicating the formation of large aggregates. These aggregates broke down easily upon stirrring with a pH probe to form a smooth suspension again. These aggregates must be quite weak and formed by the bonding of the layer agglomerates.

Leong (2024) reported that a KGa-2 suspension treated with $P_2O_7^{4-}$ additive displayed similar EDL repulsive force-control time-dependent behavior in the stepdown shear stress. The microstructure (Fig. 3a) of a diluted (15 wt.% solids) suspension treated with the same concentration (0.121 wt.%) of $P_2O_7^{4-}$ showed that most of the platelets were very thin with small platelets attached to them in the face-face configuration. The bonding between these platelets must be very strong. The interacting area, although small, must be very smooth, permitting face-face contact with a separation distance close to zero. In addition to the strong unlike charge attraction bonding them, the Vdw attraction will also be present and very strong. The Vdw attractive force is infinite in strength at zero separation distance. The microstructure also showed these thin layered agglomerates or particles (Fig. 3a) bonding among themselves in edge-face and overlapping face-face at the edge configurations. All these particles had uneven edges. The 90° edge-face attraction is rarely seen but one was highlighted.

The particle size of the KGa-2 suspensions treated with 0.121 wt.% $P_2O_7^{4-}$ was much finer than that at the natural pH, as shown by their particle-size distribution (PSD D_{50}) in Table 1. The D_{50} is 12.5% that of the untreated suspension. The D_{10}, D_{90}, surface area mean D[3,2], and volume mean D[4,3] were all significantly smaller. The $P_2O_7^{4-}$ additive caused the layered agglomerates (Leong et al., 2021c) to break up in a significant manner. It also stabilized the individual platelets and thin layered agglomerates by EDL and steric repulsive forces. Adsorbed pyrophosphate anions will also act as a steric barrier, keeping the interacting clay particles from getting too close.

The microstructure of a 15% KGa-2 suspension at pH 12.5 (Fig 3b) also showed the marked presence of very thin layered agglomerates. Again the strong face-face bond formed between small and large platelets are clearly visible. The high-pH treatment made the alumina surface strongly negative in charge. This condition is not conducive to the survival of bulky or thick layered agglomerates. Those layered agglomerates that had survived the high pH treatment must be bonded strongly with smooth surfaces. The excess OH^- ions at high pH were unable to get between the attached smooth bonding surfaces to bring about a change in the alumina surface charge. The microstructure also showed many overlapping face-face attractive interactions at the platelet edge, resulting in some cases in chain-like aggregates being formed. Low- or acute-angle edge-face attraction can also be seen. Some of the platelets were sitting at low angle from horizontal to form an edge-face bond, which were quite hard to see in this two-dimensional image. The net attractive interaction is quite weak at this pH, hence the relatively flat orientation adopted by most of the large platelets.

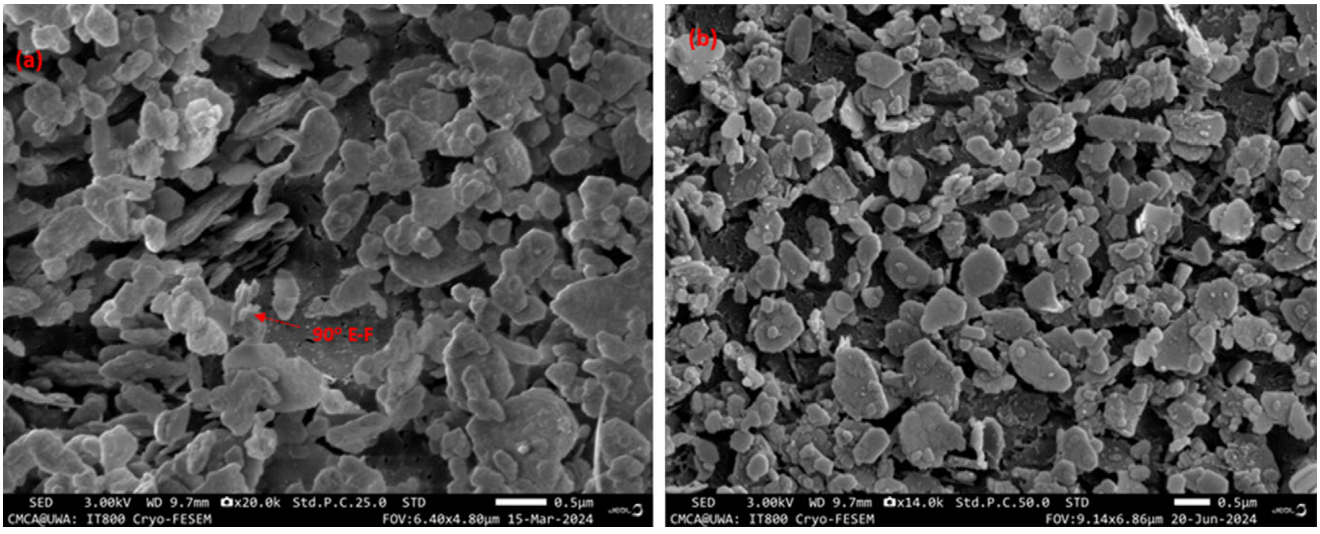

Figure 3. Microstructure of 15 wt.% KGa-2 suspensions (a) treated with 0.121 wt.% $P_2O_7^{4-}$ and (b) at pH 12.5. Thin layered agglomerates were the main species present in both images. Many of them had small platelets attached to them.

Table 1. Particle size distribution of KGa-2 suspension at its natural pH 4.53 and one treated with 0.121 wt.% $P_2O_7^{4-}$

KGa-2 suspension	D_{10} (μm)	D_{50} (μm)	D_{90} (μm)	D[4,3] (μm)	D[3,2] (μm)
pH 4.53	2.97	59.7	103	52.8	9.92
0.121 wt.% $P_2O_7^{4-}$	1.35	7.49	52.8	27.4	3.45

Ageing behavior

In the ageing test, the 31.4 wt.% KGa-2 kaolinite suspension at its natural pH did not display time-dependent behavior (Fig.4 a) even after 3 days of ageing. So were the suspensions at pH 11.0 and 11.3 (11.8 freshly made) time independent. At pH 12.5, however, marked time-dependent ageing behavior was observed. All face-face interactions must have been strongly repulsive, slowing down markedly the (+)edge-(–)face bonding process. In the linear plot (Fig. 4b), the immediate and sharp increase in the ageing yield stress is clearly more visible. However, after 1 day of ageing, a small amount of clear water was observed to form on the suspension surface, a sign of syneresis occurring.

A small amount of NaCl of 0.002 M was added to the KGa-2 suspension at pH 12.5. It caused quite a marked increase in the ageing yield stress (Fig. 4b), by about 30%. This unusual low-salt effect was also observed in hectorite gel (Leong and Clode, 2024). The added salt created more low energy paths for bonding in the (+)edge-(–)face configuration. The bonding can now occur over a wider range of angles. The bonding speed becomes faster, hastening the structural rejuvenation process. The Leong model as given by Eqn (4) described the ageing behavior of hectorite gel very well and was applied to fit the ageing data of the KGa-2 suspensions at high pH with and without salt addition. The model fits (Fig. 4b) to these two sets of ageing data were good.

The Leong model (de Kretser and Boger, 2001), which is based on a second-order particle bonding kinetics, is given by:

$$\tau_y(t) = \tau_{y_\infty}\left(1 - \frac{\left(1 - \left(\frac{\tau_{y_0}}{\tau_{y_\infty}}\right)^{3/2}\right)}{1 + K_r t}\right)^{\frac{2}{3}} \quad (4)$$

where τ_{y_0} is the yield stress at zero ageing time of the pre-sheared gel; τ_{y_∞} is the yield stress of the gel at infinite time; and $1/K_r$ is the model time constant which measures the time needed to attain $0.68\tau_{y_\infty}$. This time constant reflects the speed of the structural rejuvenation process. The assumed physics and derivation of the Leong model can be found in de Kretser and Boger (2001). They used this model to describe the ageing behavior of montmorillonite-rich coal tailings, brown coal suspensions, and bauxite residues.

The Leong model parameters (Table 2) showed a significant increase, particularly in the initial ageing yield stress by the added salt. The time constant $1/K_r$ can be used as an inverse measure of the speed of the structural rejuvenation process (Leong and Clode, 2024). A shorter time denotes a faster process. The time constant was 78 min for the salt-treated suspension and 172 min for the untreated sample. The mechanism responsible for hastening the structural rejuvenation process by the added salt should be the same as that occuring in the hectorite gel.

The electrical conductivity after salt treatment decreased slightly, from 2.96 to 2.74 mS cm^{-1}. This reduction was due to the lowering of the pH after salt treatment from pH 12.5 to 12.1. Moreover, some OH^- was replaced by Cl^-, which is less mobile. The significant increase in the gel strength by low salt treatment can be exploited in many applications such as enhancing the storage stability of kaolin-rich tailings (Leong, 2021).

The display of time-dependent behavior in ageing by the KGa-2 suspensions at high pH is a further validation of the hypothesis. An even more remarkable substantiation was the reproduction of the unusual salt effect in kaolinite suspension that occurred in the hectorite gel (Leong and Clode, 2024).

Low-defect KGa-1b suspensions

Stepdown shear rate behavior: effects of pH and $P_2O_7^{4-}$ additives

The stepdown shear rate of 40 wt.% and 50 wt.% KGa-1b kaolinite suspensions at 10 s^{-1} (Fig. 5a,b) also displayed oscillatory behavior. The amplitude and period of the cycle decreased with increasing stepdown shear rate. At 100 s^{-1}, the oscillatory behavior became less

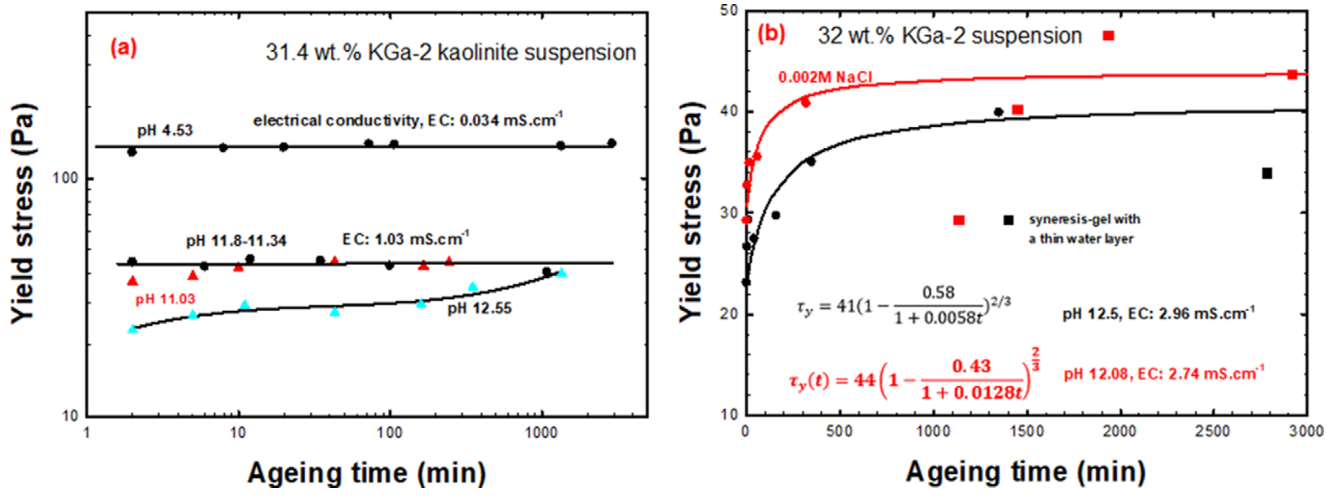

Figure 4. The ageing behavior of 31.4 wt.% KGa-2 suspension: (a) effect of pH and (b) effect of salt.

Table 2. Leong model parameters for elevated pH, 32 wt.% KGa-2 kaolinite suspension

pH	NaCl concentration (M) added	τ_{y_0} (Pa)	τ_{y_∞} (Pa)	$1/K_r$ (min)
12.5	0	23	41	172.4
12.1	0.002	30	44	78.1

discernible for the 40 wt.% solids suspension. The shear stress showed a decrease at the beginning of stepdown. This decrease became increasingly smaller at higher shear rates and disappeared completely at 300 s^{-1} for the 40 wt.% solids suspension. The shear rate must have been too high for the face-face agglomerates to form and survive. When the difference in shear stress between that just before and that just after stepdown is very large, agglomeration must have occurred in a significant manner upon stepdown. This difference is very large for the 10 s^{-1} shear rate. The significant depletion of particle by agglomeration must have occurred very quickly over a 3 s period, i.e. before the first recorded stepdown shear stress measurement. The decrease in the stepdown shear stress continued, but to a much smaller extent and for a very brief period. The trend showing a gradually increasing stepdown shear stress at 100 and 300 s^{-1} was likely due to water evaporation through the edge of the cone-and-plate during the 10 min of shearing.

Compared with KGa-2, the KGa-1b kaolinite suspensions tended to display a pronounced thixotropic behavior during shearing at 1000 s^{-1} (Fig. 5a,b). The prolonged decrease in the shear stress with time was clearly displayed despite the suspensions being agitated just before being placed in the cone-and-plate rheometer for the test. The time needed to shear at 1000 s^{-1} to reach the equilibrium state was much longer with these suspensions. The thixotropic behavior is due to the further breakdown of the structure and agglomerates, and the alignment of the kaolinite platelet in the flow direction. The KGa-2 suspension at pH >12 did display similar thixotropic behavior while being sheared at 1000 s^{-1} (Fig. 1b), but the time to reach the equilibrium state was much shorter. This high pH-treated suspension had a much lower steady shear stress or viscosity at 1000 s^{-1}. At pH >12, layered agglomerates were not formed. In this case, the thixotropic behavior characterized the progressive breakage of the (+)edge-(–)face bond and alignment of the platelets in the direction of flow. The equilibrium state of the KGa-1b suspension was reached after ~200 s of shearing. At this state, the net rate of bond breakage and formation was zero.

The imposed shear or hydrodynamic force is responsible for the shear thinning thixotropic behavior, i.e. breaking the particle bonds and aligning the anisotropic particles in the flow direction. This required the particles to form a bond and network structure. The nature of the attractive colloidal force responsible for bonding is not important. It can be Vdw or the unlike charge attraction, or both. This thixotropic behavior becomes visible only when the bond breakage and the anisotropic particle flow alignment processes occurred over an observable time scale. When the particle bond is very weak, such behavior may not be observable. In structural rejuvenation, a specific colloidal force is responsible for the time-dependent behavior. There are no other forces to complicate the analysis and understanding. The identification of this force required the formulation of a highly plausible mechanism based on strong experimental evidence (Leong and Clode, 2023; Leong, 2024). The attractive force that caused the platelets to bond and form progressively stronger network structure with time is not responsible for the time-dependent behavior. The repulsive force that slowed down this bonding process is. A structural rejuvenated gel will display thixotropic behavior upon shearing, and this is the relationship between the two.

The addition of 0.026 wt.% $P_2O_7^{4-}$ caused the 40 and 50 wt.% KGa-1b suspensions to display time-dependent behavior (Fig. 6) in the stepdown shear stress response. This EDL repulsive force-control time-dependent behavior, characterized by the stepdown shear stress increasing with time, was markedly exhibited. The elimination of alumina-silica face-face attraction and the enhancement of EDL repulsion in all face-face interactions by the adsorbed $P_2O_7^{4-}$ were responsible. Steric repulsive force arising from the adsorbed $P_2O_7^{4-}$ also contributed to the slowing down of the bonding process. A similar time-dependent behavior was reproduced by the 40 wt.% solids suspension kept overnight. The magnitude of the stepdown shear stress was higher, however. The equilibrium shear stress at 1000 s^{-1} was also much higher.

Raising the pH to an adequate level also caused the KGa-1b suspensions to display time-dependent behavior (Fig. 7) in the stepdown shear stress response. This EDL repulsive force-control time-dependent behavior was displayed by 40, 45, and 50 wt.% suspensions when the pH was more than 9. At higher pH such as ~10 and ~11, this behavior became more marked. This display occurred at a much lower pH compared with that obtained with the KGa-2 suspension, by 2–3 pH units lower. At pH 10, the negative charges acquired by the alumina surface must be sufficient to produce the strong EDL face-face repulsion in the KGa-1b suspensions. Similarly, the concentration of $P_2O_7^{4-}$ required to produce this time-dependent behavior was also much lower. As the positive layer charge in the octahedral or alumina sheet is much lower, either a smaller amount of $P_2O_7^{4-}$ or a lower pH elevation was sufficient to make all the face-face interactions

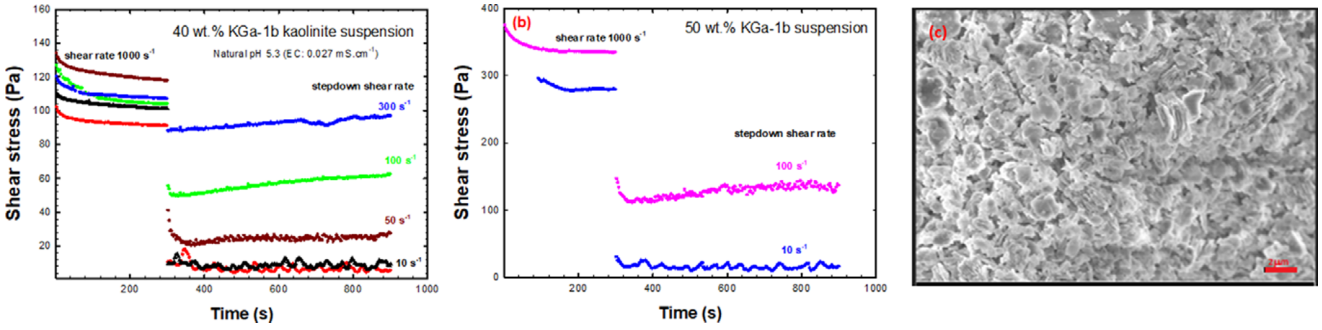

Figure 5. The stepdown shear rate behavior of KGa-1b kaolinite suspension at different shear rates for (a) 40 wt.% and (b) 50 wt.% solids; (c) microstructure of 45 wt.% KGa-1b suspension at its natural pH showing the presence of layered agglomerates.

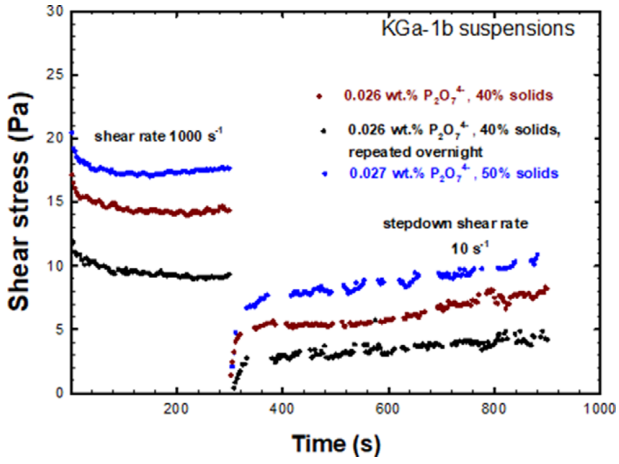

Figure 6. The stepdown shear rate behavior of 40 and 50 wt.% KGa-1b suspensions with 0.026 wt.% $P_2O_7^{4-}$ (or g of $P_2O_7^{4-}$ per 100 g clay solids). The 40 wt.% suspension was recharacterized overnight.

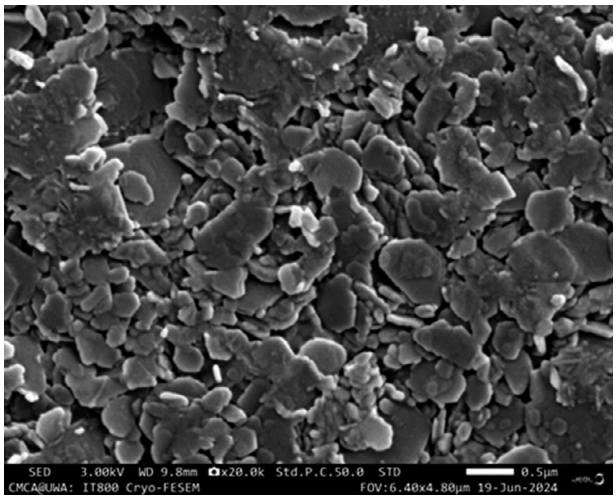

Figure 8. The microstructure of 21.7 wt.% KGa-1b suspension at its natural pH 5.3 showed the presence of face-face agglomerates; (+)edge-(–)face attraction of layered agglomerates forming the network structure in a more concentrated suspension is more clearly seen in Leong et al. (2021c).

repulsive. The KGa-1b has a positive layer charge of 0.11 e compared with 0.16 e for the KGa-2. A lower alkaline pH is thus needed to first neutralize the KGa-1b layer charge and then to make the alumina surface sufficiently negative to produce the strong EDL face-face repulsion. Similarly, less $P_2O_7^{4-}$ is needed to neutralize the positive layer charge and still have enough to make the alumina face sufficiently negative. The amount of $P_2O_7^{4-}$ required was ~4 times smaller, 0.026 wt.% $P_2O_7^{4-}$ for the KGa-1b and ~0.1 wt.% $P_2O_7^{4-}$ for the KGa-2 (Leong, 2024). The specific surface area of KGa-2 is only two times larger, and so the higher number of charge sites cannot account for the difference in the amount of $P_2O_7^{4-}$ needed.

The KGa-1b suspensions used in the cryo-SEM FESEM imaging were more dilute than that used in the rheological test. The nature of the platelet or particle interaction configurations should remain the same, irrespective of the suspension concentration at the same surface chemistry condition: pH, salt concentration, and adsorbed additive concentration. The bonding density will thus be lower.

The kaolinite particles at its natural pH of 5.3 existed mainly as layered agglomerates (Fig. 8). These agglomerates with uneven edges interact attractively via (+)edge-(–) silica face to form the network structure (Leong et al., 2021c). At pH 10.9, the microstructure (Fig. 9) of a 22 wt.% solids suspension showed the presence of many platelets with very smooth surfaces. Attached small particles were present on these surfaces but only a handful can be seen. The high-pH treatment must have brought about significant detachment of bonded platelets of the layered agglomerates as the alumina surface is now sufficiently negative to destabilize such bonds. At this pH, the display of marked time-dependent behavior in the stepdown shear stress was observed.

The microstructure (Fig. 10) of a 25 wt.% KGa-1b suspension treated with 0.027 wt.% $P_2O_7^{4-}$ showed the presence of relatively large, layered agglomerates. The $P_2O_7^{4-}$ was not at a sufficient concentration to reduce all the agglomerates into individual platelets and the particle-size distribution result provided further support. Most were face-face agglomerates. Some were layered with large platelets. Most had a handful of small platelets or particles attached to the surface. The size of most agglomerates was of the order of ~1 µm. The additive was, however, sufficient to weaken attractive interaction between the kaolinite particles considerably and this was reflected by the low shear stress obtained (Fig. 7).

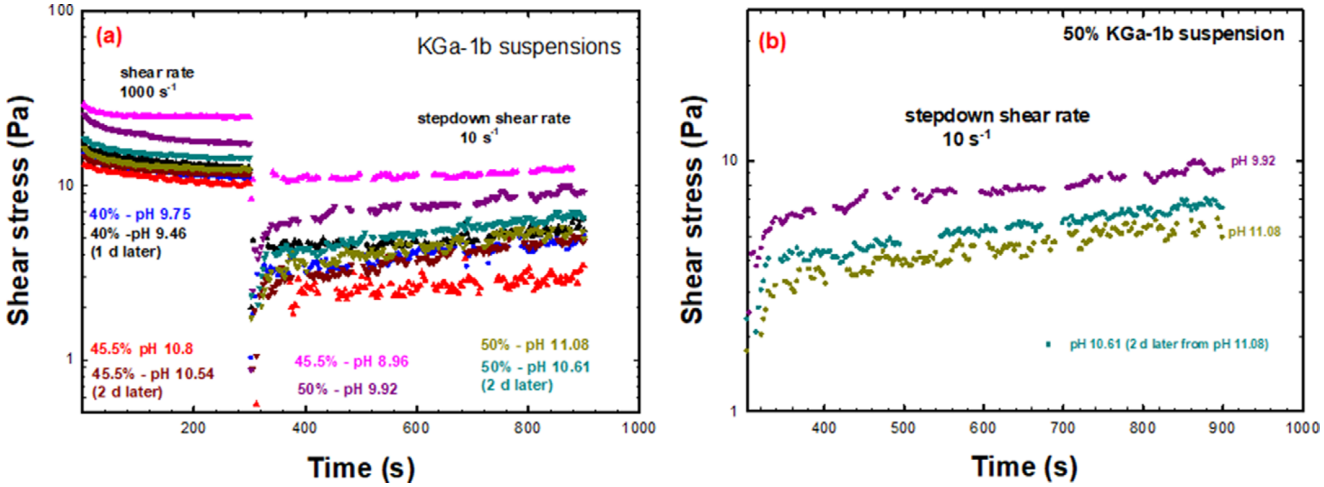

Figure 7. The stepdown shear rate behavior of KGa-1b suspensions at high pH levels: (a) 40 wt.% solids and (b) 50 wt.% solids.

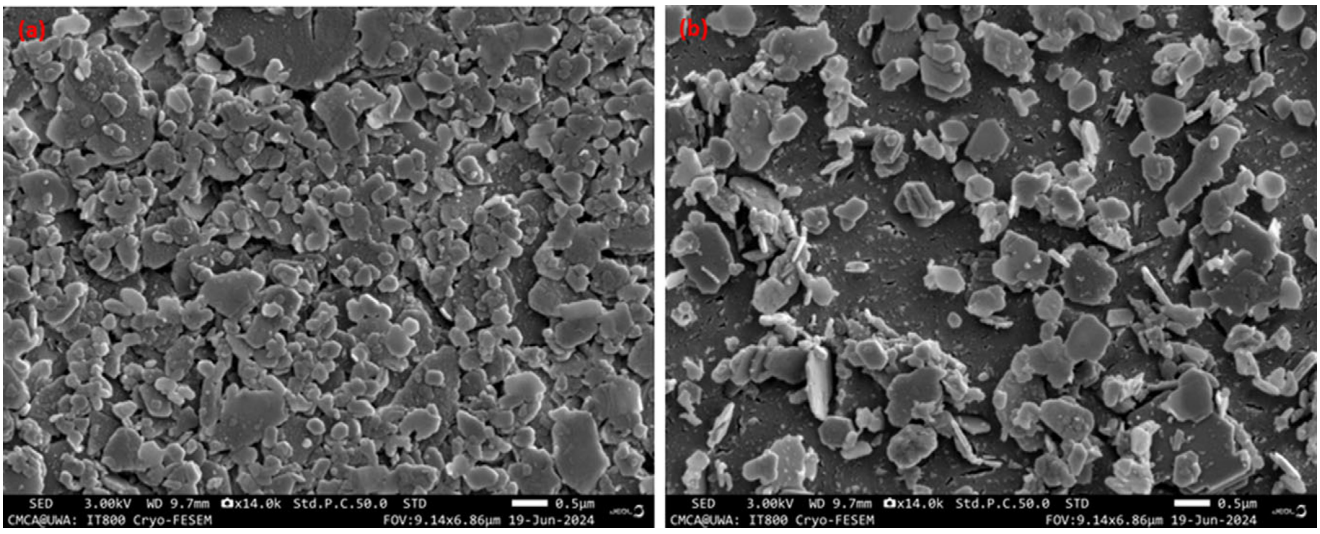

Figure 9. The microstructure of 22 wt.% KGa-1b suspension at pH 10.9: (a) high density of platelets with small platelets attached to them and (b) less dense region with lots of smooth face platelets.

The PSD in Table 3 showed that treated KGa-1b suspensions at pH 10.9 and with 0.027 wt.% $P_2O_7^{4-}$ were much finer than the suspension at its natural pH based on the D_{10} and D_{50} data. Two samples treated with the same concentration of $P_2O_7^{4-}$ were characterized, one at 25 wt.% solids used in the cryo-SEM imaging and the other at 50 wt.% solids used in the stepdown shear rate test. Their PSD differed quite markedly in D_{90} and the volume mean D[4,3]. The D_{90} of all the treated suspensions were also smaller except for an anomaly displayed by the 25 wt.% suspension treated with $P_2O_7^{4-}$. The cryo-SEM images of this suspension in Fig. 10 also showed the presence of a considerable proportion of layered agglomerates. Nevertheless, a marked reduction of the layered agglomerate size was clearly achieved by these elevated pH and $P_2O_7^{4-}$ treatments. As a result of these treatments, individual platelets and thinner layered agglomerates were formed in the suspension. Surface forces such as EDL repulsive and (+)edge-(–)face attractive forces are important for smaller colloidal agglomerates.

Flow behavior – effect of logarithmic time step in the stepdown shear rate

It is common to characterize the flow behavior of concentrated suspension in the direction of high to low shear rate. It is also normal to shear the suspension to an equilibrium state at a high shear rate before performing the flow characterization. The state of the suspension at the start of the flow characterization is thus well-defined. In this state, the network structure no longer exists and the anisotropic particles are aligned in the flow direction. The speed at which the flow characterization performed particularly in the low shear rate region will affect the quantity and size of the layered agglomerates formed and, therefore, the flow behavior obtained. In this investigation, the effect of time employed in the flow behavior characterization of a 40 wt.% solids KGa-1b suspension was evaluated. The direction of the characterization was from 1000 to 1 s^{-1} and logarithmic ramp mode was chosen for the 30 shear rate steps. A range of time to complete the flow characterization was selected. For each, the characterization time at each shear rate will

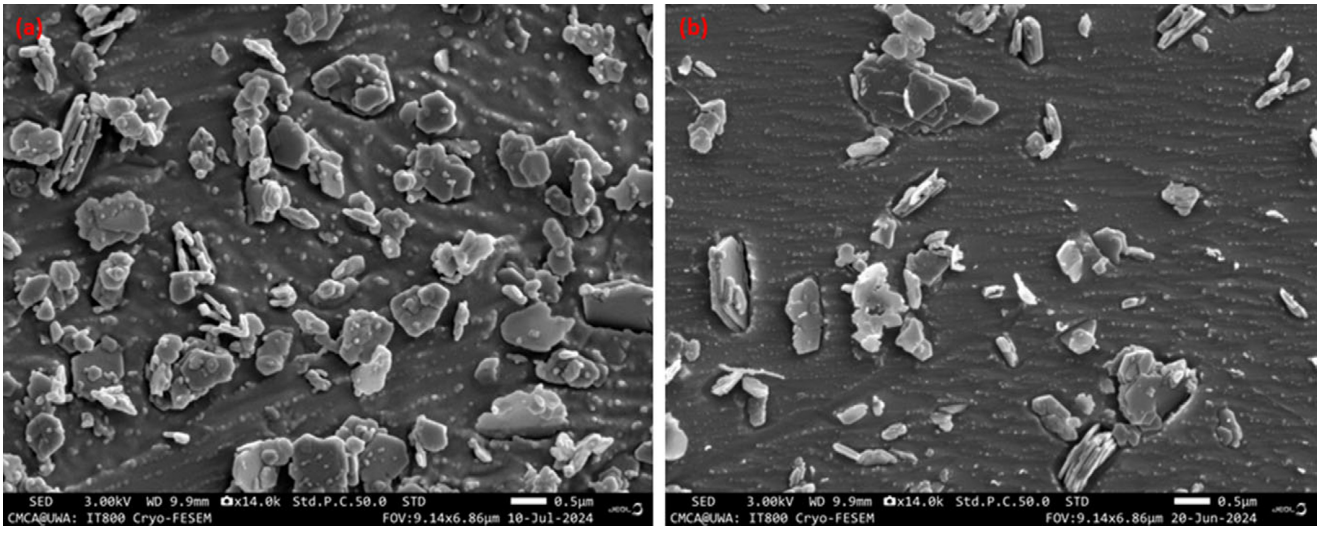

Figure 10. The microstructure of 25 wt.% KGa-1b suspension with 0.027 wt.% $P_2O_7^{4-}$: (a) high platelet density and (b) layered aggregates present. The underlying materials are vitreous or amorphous ice formed by high pressure freezing (HPF). Not all the ice was sublimed in the sample for the coating process.

Table 3. Particle-size distribution of KGa-1b suspensions at its natural pH 5.3, pH 10.9, and treated with 0.027 wt.% $P_2O_7^{4-}$

KGa-1b suspension	D_{10} (μm)	D_{50} (μm)	D_{90} (μm)	D[4,3] (μm)	D[3,2] (μm)
Natural pH 5.3	2.87	6.65	21.2	15.9	5.6
pH 10.9	1.0	4.0	19.3	7.42	2.39
0.027 wt.% $P_2O_7^{4-}$ (25% solids)	1.64	4.33	24.2	24.1	3.38
0.027 wt.% $P_2O_7^{4-}$ (50% solids)	1.04	3.28	15.2	5.85	2.31

be the same. A shearing time of 300 s at 1000 s^{-1} was sufficient for the suspension to reach the equilibrium or steady state (Fig. 11a) as reflected by the shear stress being constant for all samples after 300 s of shearing. The time employed to complete the flow characterization was varied from 10 to 300 s. The flow curves (Fig. 11b) showed that the shear stress was relatively flat in the low shear rate region below 10 s^{-1}. The shear stress in this region, as predicted, showed sensitivity to the duration of the flow characterization. For the shortest time of 10 s (0.55 s per step for 18 shear rate steps), the value of this shear stress is highest. It is lowest for the 300 s (10 s per step for 30 shear rate steps). At the characterization time of 10 s, the platelets do not have time to agglomerate in the low shear rate region, leaving a high concentration of particles to contribute to the viscosity or shear stress via hydrodynamic, repulsive and attraction interactions and, hence, the higher shear stress values. At long characterization time, many particles were sequestered to form the compact agglomerates reducing the number of particles in the suspension. A contradicting result was obtained for the 600 s flow characterization time. The higher shear stress in the low shear rate region was due to the drying out of the suspension during the characterization. This suspension would have spent at least 15 min being sheared in the cone-and-plate rheometer. The high sensitivity of the torque measurement meant a small drier lump at the cone-and-plate edge can give rise to a markedly higher shear stress.

The flow behavior displayed by the KGa-1b suspension obtained in this manner was quite unusual. It had a highly reproducibility Newtonian region in the shear rate range of between 50 and 100 s^{-1}. The flow data in the range of 70–1000 s^{-1} were not affected by the

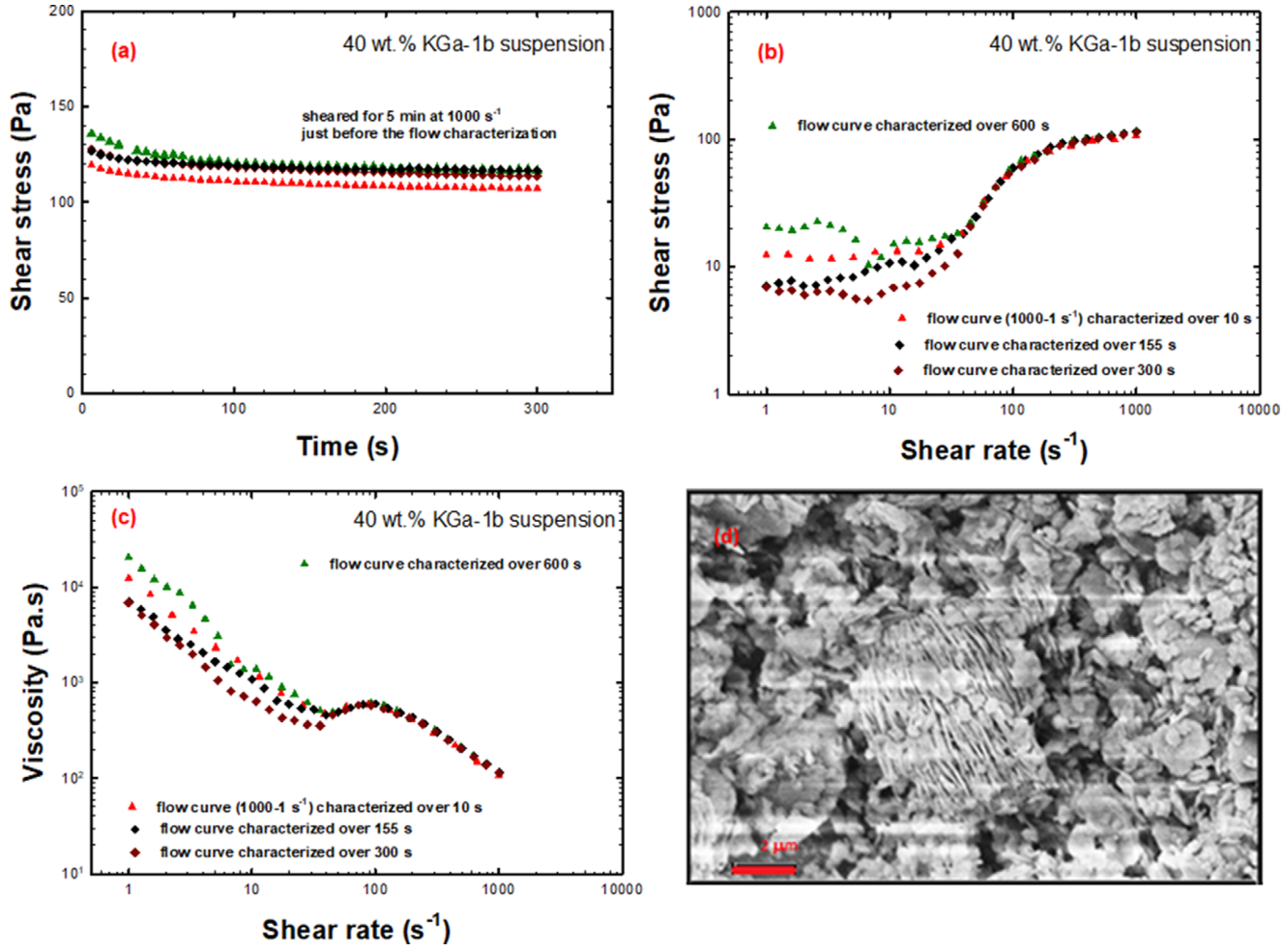

Figure 11. Flow behavior characterization of KGa-1b suspension. (a) Attainment of equilibrium state at 1000 s^{-1} and then (b) followed by the flow characterization via progressive step down in the shear rate using a range of logarithmic time step. (c) The corresponding viscosity-shear rate plots. (d) An example of large face-face agglomerates with edge-face attraction with smaller platelets – this cryo-SEM image was captured a few years later using a different brand of equipment.

duration of measurement at each shear rate step. This suggests that the platelet agglomeration was not important in this shear rate region. Any agglomerates formed will be too weak to withstand the hydrodynamic stress of the flow.

Iron ore tailings

The iron ore tailings used contained a large amount of colloidal kaolinite and goethite (Leong, 2021). Like the kaolinite suspension, these tailings did not display time-dependent behavior in the ageing yield stress (Fig. 12a). There was no immediate increase in the yield stress at the start of ageing. Syneresis occurred and a layer of clear water was found on the tailings surface after ~1 day rest. Increasing the tailings pH and the use of $P_2O_7^{4-}$ additive did cause the tailings to display time-dependent behavior in ageing (Fig. 12a). Similarly, in the stepdown shear rate mode (Fig. 12b,c), these tailings displayed time-dependent behavior when the pH was raised to 9.4 and when 0.049 and 0.076 wt.% $P_2O_7^{4-}$ were added. A magnified stepdown shear stress response was also shown (Fig. 12c). The tailings rheological behavior was successfully modified in a manner as predicted. Using the knowledge learned, time-dependent properties were imparted to a mineral processing plant waste product. This is another piece of evidence validating the hypothesis. This manipulation of tailing properties has a practical application. It can be used to enhance the safe storage of tailings. The reduction in the tailing viscosity or yield stress by increasing the pH or the use of adsorbed anionic additives reduced the transport cost of pumping the tailings to a storage facility or dam. Some dams are located several kilometres away from the processing plant. At the dam, the spontaneous structural rejuvenation process will form a stronger network structure with time, imparting a relatively high yield stress property to tailings.

Conclusions

For KGa-1b and KGa-2 suspensions to display time-dependent behavior in the structural development or rejuvenation phase, the premise that all the face-face interactions must be strongly repulsive has proven to be correct. This includes the alumina face and silica face interaction which is attractive at low pH. To make this face-face interaction repulsive, the alumina octahedral sheet face charge was made strongly negative. Two methods, the use of adsorbing $P_2O_7^{4-}$ anions and high pH treatment, were demonstrated to be very successful. These two treatments at the right conditions, would have produced enough negative charges to neutralize the positive octahedral layer charge and still have enough to impart a significant negative charge to the alumina surface. The amount of $P_2O_7^{4-}$ needed and the extent of pH elevation required were much larger for the low-crystallinity KGa-2 kaolinite, which has a much larger positive layer charge in the octahedral sheet, than for the KGa-1. The strong face-face repulsion slowed down the (+)edge-(–)face bonding considerably, and hence also the display of visible time-dependent behavior.

KGa-2 and KGa-1b suspensions at their natural pH of 4.5 and 5.3, respectively, displayed an oscillatory stepdown shear stress response. This oscillatory behavior was eliminated when (i) all fixed-charge interactions were made unimportant by high salt concentration (0.5 M KCl) and (ii) all the face-face interactions were made repulsive by elevating the pH sufficiently. This confirmed that the layered agglomerate formed during stepdown was the cause of the oscillatory behavior. High stepdown shear rates

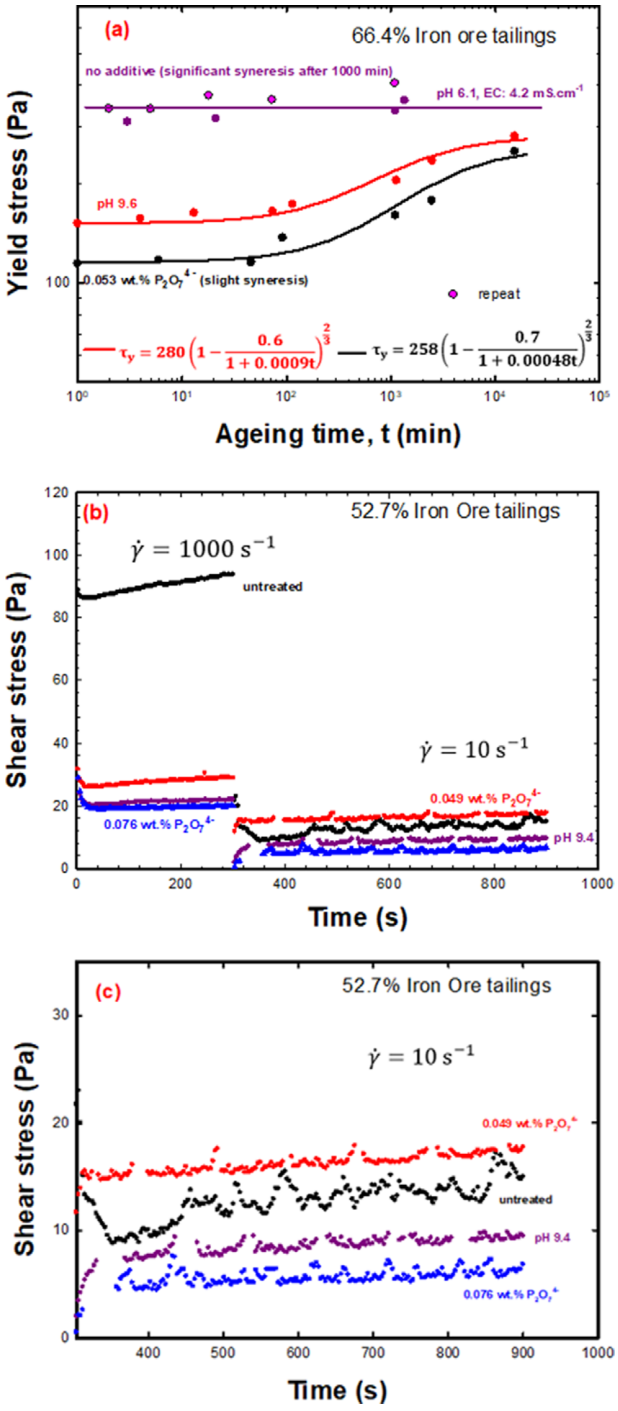

Figure 12. (a) The ageing behavior of iron ore tailings with and without pH or $P_2O_7^{4-}$ treatments. (b) The stepdown shear rate test of filtered 52.7 wt.% iron ore tailings (pH 6.01, EC 0.42 mS cm^{-1}) behavior showing stress response at high and low shear rate. (c) The stepdown shear stress response of iron ore tailings; untreated, at elevated pH, and at two different $P_2O_7^{4-}$ concentrations.

of 100–300 s^{-1} also caused the oscillatory behavior to disappear. At 0.5 M KCl, only the van der Waals forces are important.

The platelet bonding process was hastened by a small amount of salt, 0.002 M NaCl, added to a high-pH KGa-2 suspension speeding up the structural rejuvenation process. The magnitude of the ageing yield stress was also larger than that before the salt treatment. This speeding up of the structural rejuvenation process and the

strengthening of platelet bond by the low-salt treatment were also observed with hectorite clay gels. The salt essentially affects the strength and the configuration of the (+)edge-(–)face bond. The Leong model time constant can be used as a measure of the speed of this structural rejuvenation process.

Data availability statement. Data will be made available upon request.

Acknowledgments. The authors acknowledge Dr Sam Gunasekera for technical assistance and use of the cryoSEM facilities of Microscopy Australia within the Centre for Microscopy, Characterisation and Analysis at UWA, a facility funded by the University plus State and Commonwealth Governments. Professor Paul McCormick is also thanked for intellectual discussions on the possible cause of the oscillatory stepdown shear stress behavior. The authors thank the reviewers and editors for making this a better paper.

Author contribution. YKL came up with the theory and the experimental design to verify the hypothesis. He also performed all the rheological experiments, analysis and write the paper. PLC was responsible for the microstructure imaging and wrote the experimental part of the cryo-SEM imaging.

Competing interests. The authors declare no competing interests.

References

Au, P.I., Clode, P., Smart, R.St.C., & Leong, Y.K. (2015). Surface chemistry-microstructure-rheology of high and low crystallinity KGa-1b and KGa-2 kaolinite suspensions. *Colloids and Surfaces A: Physicochemical and Engineering Aspects*, *484*, 354–364. https://doi.org/10.1016/j.colsurfa.2015.08.013

Bergaya, F., Theng, B.G.K., & Lagaly, G. (2006). *Handbook of Clay Science*. Elsevier.

CMS (2024). *Physical and Chemical Data of Source Clays*. https://www.clays.org/sourceclays_data/

de Bono, J., & McDowell, G. (2023). Simulating multifaceted interactions between kaolinite platelets. *Powder Technology*, *413*, 118062. https://doi.org/10.1016/j.powtec.2022.118062

de Kretser, R.G., & Boger, D.V. (2001). A structural model for the time-dependent recovery of mineral suspensions. *Rheologica Acta*, *40*, 582–590. https://doi.org/10.1007/s003970100180

Franks, G.V. (2002). Zeta potentials and yield stresses of silica suspensions in concentrated monovalent electrolytes: isoelectric point shift and additional attraction. *Journal of Colloid and Interface Science*, *249*, 44–51. https://doi.org/10.1006/jcis.2002.8250

Gupta, V., Hampton, M.A., Stokes, J.R., Nguyen, A.V., & Miller, J.D. (2011). Particle interactions in kaolinite suspensions and corresponding aggregate structures. *Journal of Colloid Interface Science*, *359*, 95–103. https://doi.org/10.1016/j.jcis.2011.03.043

Harvey, C.C., & Murray, H.H. (1997). Industrial clays in the 21st century: a perspective of exploration, technology and utilization. *Applied Clay Science*, *11*, 285−310.

Israelachvili, J.N. (1992). *Intermolecular and Surface Forces*. Academic press.

Kosmulski, M. (2023). The pH dependent surface charging and points of zero charge. X. Update. *Advances in Colloid and Interface Science*, *319*, 102973. https://doi.org/10.1016/j.cis.2023.102973

Kumar, N., Andersson, M.P., van den Ende, D., Mugele, F., & Siretanu, I. (2021). Probing the surface charge on the basal planes of kaolinite particles with high-resolution atomic force microscopy. *Langmuir*, *33*, 14226–14237. https://doi.org/10.1021/acs.langmuir.7b03153

Leong, Y.K. (2021). Controlling the rheology of iron ore slurries and tailings with surface chemistry for enhanced beneficiation performance and output, reduced pumping cost and safer tailings storage in dam. *Minerals Engineering*, *166*, 106874. https://doi.org/10.1016/j.mineng.2021.106874

Leong, Y.K. (2024). Direct evidence of electric double layer (EDL) repulsive force being responsible for the time-dependent behavior of clay gels in the structural rejuvenation mode. *Journal of Physical Chemistry B*, *128*, 3784−3793. https://doi.org/10.1021/acs.jpcb.4c00858

Leong, Y.K., & Clode, P.L. (2023). Time-dependent clay gels: stepdown shear rate behavior, microstructure, ageing, and phase state ambiguity. *Physics of Fluids*, *35*, 123329. https://doi.org/10.1063/5.0167806

Leong, Y.K., & Clode, P.L. (2024). Unusual salt effects on the time-dependent behavior of charge and shape anisotropic hectorite clay gels: role of electric double layer (EDL) repulsive force. *Journal of Chemical Physics*, *161*, 224906. https://doi.org/10.1063/5.0241130

Leong, Y.K., Liu, P., Au, P.I., Clode, P., & Liu, J. (2021a). Microstructure and time-dependent behavior of STx-1b calcium montmorillonite suspensions. *Clays and Clay Minerals*, *69*, 787–796. https://doi.org/10.1007/s42860-021-00170-5

Leong, Y. K., Liu, P., Clode, P., & Liu, J. (2021b). Ageing behavior spanning months of NaMt, hectorite and Laponite gels: surface forces and microstructure – a comprehensive analysis. *Colloids and Surfaces A: Physicochemical and Engineering Aspects*, *630*, 127543. https://doi.org/10.1016/j.colsurfa.2021.127543

Leong, Y.K., Liu, P., Au, P.I., & Clode P. (2021c). Microstructure of KGa-1b and KGa-2 kaolin suspensions revisited. *Colloids and Surfaces A: Physicochemical and Engineering Aspects*, *617*, 126354. https://doi.org/10.1016/j.colsurfa.2021.126354

Liu, D., Edraki, M., Fawell, P., & Berry, L. (2020). Improved water recovery: review of clay-rich tailings and saline water interactions. *Powder Technology*, *364*, 604–621. https://doi.org/10.1016/j.powtec.2020.01.039

Liu, X., Lu, X., Sprik, M., Cheng, J., Meijer, E.J., & Wang, R. (2013). Acidity of edge surface sites of montmorillonite and kaolinite. *Geochimica et Cosmochimica Acta*, *117*, 180–190. https://doi.org/10.1016/j.gca.2013.04.008

Murray, H.H. (2000). Traditional and new applications for kaolin, smectite, and palygorskite: a general overview. *Applied Clay Science*, *17*, 207–221. https://doi.org/10.1016/S0169-1317(00)00016-8

Palomino, A.M., & Santamarina, J.C. (2005). Fabric map for kaolinite: effects of pH and ionic concentration on behavior. *Clays and Clay Minerals*, *53*, 211–223. https://doi.org/10.1346/CCMN.2005.0530302

Rand, B., & Melton, I.E. (1977). Particle interactions in aqueous kaolinite suspensions: I. Effect of pH and electrolyte upon the mode of particle interaction in homoionic sodium kaolinite suspensions. *Journal of Colloid Interface Science*, *60*, 308–320. https://doi.org/10.1016/0021-9797(77)90290-9

Schofield, R.K., & Samson, H.R. (1954). Flocculation of kaolinite due to the attraction of oppositely charged crystal faces. *Discussions of the Faraday Society*, *18*, 135–145. https://doi.org/10.1039/DF9541800135

Swartzen-Allen, L., & Matijević, E. (1974). Surface and colloid chemistry of clays. *Chemical Review*, *74*, 385–400. https://doi.org/10.1021/cr60289a004

van Olphen, H. (1963). *Introduction to Clay Colloid Chemistry*. Interscience, New York.